π^0 and η meson exchange interactions in the coherent η meson production in the nucleus

Swapan Das [1]
Nuclear Physics Division, Bhabha Atomic Research Centre
Mumbai-400085, India

Abstract

The energy transfer spectra have been calculated for the coherent η meson production in the proton nucleus reaction. The elementary reaction occurring in the nucleus is considered as $pN \to pN^*(1535)$; $N^*(1535) \to N\eta$. The $N^*(1535)$ excitation for the forward going proton and η meson is occurred due to the π^0 and η meson exchange interactions, other mesons do not contribute in this process. The cross sections are calculated for the π^0 and η meson exchange interactions, and the effect of their interference on the cross section is also studied. The initial and final state interactions as well as the $N^*(1535)$ nucleus interaction are addressed by the optical potentials. The distorted wave functions for proton and η meson are described by the eikonal form. The sensitivity of the cross section to the hadron nucleus potential is presented.

Keywords: η meson production, π^0 and η meson exchange interactions, hadron nucleus optical potentials

PACS number(s): 25.40e, 13.30.Eg, 13.60.Le

1 Introduction

One of the current interests in the intermediate energy nuclear physics is to explore the physics of η meson [1]. Several data sets for the η meson production in the hadron induced reactions have been available from various laboratories, like COSY [2] (see the references there in), SATURNE [3], Los Alamos [4], Brookhaven [5]. The η meson production in the heavy-ion collisions is reported from GSI [6]. Due to the advent of the high duty electron accelerators at Jefferson Laboratory, Bates, MAMI, ELSA, ... etc, good quality data for the photo- and electro- production of the η meson are also available [7]. These accelerator facilities, along with the newly developed sophisticated detecting systems, provide ample scope to explore the dynamics of the η meson in the nuclear and particle reactions.

The study of the η meson production reaction opens various avenues to learn many exciting physics. The ηN scattering length near threshold is large and attractive which predicts the existence of a new type of hadronic atom, i.e., bound or quasi-bound eta mesic

[1]email: swapand@barc.gov.in

nucleus [8, 9, 10]. Large charge symmetry violation in the $\pi^0 - \eta$ mixing [11] provides a way to estimate the mass difference between u and d quarks. Being an isoscalar particle, the η meson can excite a nucleon to a $I = \frac{1}{2}$ nucleonic resonance. Specifically, the η meson strongly couples only to $N^*(1535)$, a $I(J^P) = \frac{1}{2}(\frac{1}{2}^+)$ nucleonic resonance. Therefore, the η meson production in the nuclear reaction is a potential tool to investigate the propagation of the $N^*(1535)$ resonance in the nucleus, in addition to the study of the η meson nucleus interaction in the final state [12, 13].

The η meson can be produced through the hadronic interaction by scattering of the pion or proton off the proton or nuclear target. Theoretical studies on these reaction, as done by various authors [14, 15, 16], show that the η meson in the final state arises due to the decay of $N^*(1535)$ resonance produced in the intermediate state. Sometime back, Alvaredo and Oset [17] studied the coherent η meson production in the (p, p') reaction in the spin-isospin saturated nucleus: $p + A(gs) \rightarrow p' + A(gs) + \eta$. The elementary reaction in the nucleus proceeds as $pN \rightarrow pN^*$; $N^*(1535) \rightarrow N\eta$. The $N^*(1535)$ resonance produced in the intermediate state due to the η meson (a psuedoscalar-isoscalar meson) exchange interaction only, specifically, for the forward going proton and η meson. The contributions from other meson exchange interactions vanish in this reaction [17].

It could be mentioned that both π and η mesons are pseudoscalar particles but pion can't contribute to above reaction since it is an isovector meson and this reaction involves isoscalar nucleus. Contrast to this, both π and η meson exchange interactions contribute to $p \rightarrow N^*(1535)$ excitation in the spin-saturated isospin-one nucleus. We, therefore, consider the coherent η meson production in the scalar-isovector nucleus through the (p, p') reaction, and study the contributions due to the π^0, η meson exchange interactions and the interference of these interactions. The diagrammatic presentation of the elementary reaction occurring in the nucleus is presented in Fig. 1. It should be mentioned that the η meson takes away almost the whole energy transferred to the nucleus, i.e., $E_\eta \approx q_0 [= E_p - E_{p'}]$, whereas the momentum of this meson is adjusted by the recoiling nucleus. The distorted wave functions of protons and η meson are described by the eikonal form. The optical potentials (appearing in the N^* propagator and the distorted wave functions for protons) are evaluated using the "$t\varrho(\mathbf{r})$" approximation. We take the η meson nucleus optical potential from Ref. [17].

2 Formalism

The Lagrangian densities describing the πNN, πNN^*, ηNN and ηNN^* interactions [18] are given by

$$\begin{aligned} \mathcal{L}_{\pi NN} &= -ig_\pi F_\pi(q^2) \bar{N} \gamma_5 \tau N \cdot \pi \\ \mathcal{L}_{\pi NN^*} &= -g^*_\pi F^*_\pi(q^2) \bar{N}^* \tau N \cdot \pi \end{aligned}$$

$$\begin{aligned}\mathcal{L}_{\eta NN} &= -ig_\eta F_\eta(q^2)\bar{N}\gamma_5 N\eta \\ \mathcal{L}_{\eta NN^*} &= -g^*_\eta F^*_\eta(q^2)\bar{N}^* N\eta, \end{aligned} \tag{1}$$

where $g_{\pi(\eta)}$ and $g^*_{\pi(\eta)}$ denote the $\pi(\eta)NN$ and $\pi(\eta)NN^*$ coupling constants respectively. The values for them are $g_\pi = 13.536$, $g^*_\pi = 0.79$, $g^*_\eta = 2.22$ and $g_\eta = 7.927$ [9, 16, 19]. $F_{\pi(\eta)}$ and $F^*_{\pi(\eta)}$ are the $\pi(\eta)NN$ and $\pi(\eta)NN^*$ form factors which are given by

$$F_M(q^2) = F^*_M(q^2) = \frac{\Lambda^2_M - m^2_M}{\Lambda^2_M - q^2}; \qquad (M = \pi^0, \eta). \tag{2}$$

$q^2[= q_0^2 - \mathbf{q}^2]$ is the four-momentum transfer from pp' vertex to the nucleus, i.e., $q_0 = E_p - E_{p'}$ and $\mathbf{q} = \mathbf{k}_p - \mathbf{k}_{p'}$. The form factors are normalized to unity when the mesons are in on-shell. Values for the length parameters are $\Lambda_\pi = 1.3$ GeV and $\Lambda_\eta = 1.5$ GeV [9, 19]. m_M denotes the mass of the pseudoscalar meson: $m_{\pi^0} \simeq 135$ MeV and $m_\eta \simeq 547$ MeV.

The T-matrix for the coherent η production in the (p, p') reaction on a nucleus can be written as

$$T_{fi} = \hat{\Gamma}_{N^*\to N\eta} \sum_{M=\pi^0,\eta} \tilde{V}_M(q) \int d\mathbf{r}\chi^{(-)*}(\mathbf{k}_\eta, \mathbf{r})G_{N^*}(m, \mathbf{r})\varrho(\mathbf{r})\chi^{(-)*}(\mathbf{k}_{p'}, \mathbf{r})\chi^{(+)}(\mathbf{k}_p, \mathbf{r}), \tag{3}$$

where $\varrho(\mathbf{r})$ is the density distribution of the nucleus. $\hat{\Gamma}_{N^*\to N\eta}$ denotes the decay vertex: $N^*(1535) \to N\eta$. $V_M(q)$ is the pseudoscalar meson (i.e., $M \equiv \pi^0$ or η) exchange interaction between the beam proton and the nucleon in the nucleus (see Fig. 1). It is given by

$$\tilde{V}_M(q) = \hat{\Gamma}_{MNN^*}\tilde{G}_M(q^2)\hat{\Gamma}_{Mpp'}. \tag{4}$$

$\hat{\Gamma}_{MNN^*}$ and $\hat{\Gamma}_{Mpp'}$ appearing in this equation represent the $\pi(\eta)NN^*$ and $\pi(\eta)pp'$ vertex factors. They are described by the Lagrangians expressed in Eq. (1). $\tilde{G}_M(q^2)$ in the above equation denotes the propagator arising due to the virtual $\pi(\eta)$ meson exchange interaction. The form for it is

$$\tilde{G}_{\pi(\eta)}(q^2) = -\frac{1}{m^2_{\pi(\eta)} - q^2}. \tag{5}$$

χs in Eq. (3) represent the distorted wave function for the projectile p, ejectile p' and η meson. Using Glauber model [20], we can write χ for the beam proton p [21] as

$$\chi^{(+)}(\mathbf{k}_p, \mathbf{r}) = e^{i\mathbf{k}_p\cdot\mathbf{r}} exp[-\frac{i}{v_p}\int_{-\infty}^{z} dz' V_{Op}(\mathbf{b}, z')], \tag{6}$$

where v_p is the velocity of the proton. $V_{Op}(\mathbf{b}, z')$ describes the optical potential for it. For outgoing particles, i.e., p' and η meson, the form for their distorted wave functions is given by

$$\chi^{(-)^*}(\mathbf{k}_X, \mathbf{r}) = e^{-i\mathbf{k}_X.\mathbf{r}} exp[-\frac{i}{v_X}\int_z^{+\infty} dz' V_{OX}(\mathbf{b}, z')], \qquad (X = p', \eta). \tag{7}$$

The optical potentials appearing in the above equations describe the initial and final state interactions.

The propagator of the N^* baryon, i.e., $G_{N^*}(m, \mathbf{r})$ in Eq. (3), can be expressed as

$$G_{N^*}(m, \mathbf{r}) = \frac{2m_{N^*}}{m^2 - m_{N^*}^2 + im_{N^*}\Gamma_{N^*}(m) - 2E_{N^*}V_{ON^*}(\mathbf{r})}, \tag{8}$$

with $m_{N^*} = 1.535$ GeV. E_{N^*} is the energy of N^* resonance. m represents the invariant mass of the η meson and nucleon, arising due to the decay of N^*. $V_{ON^*}(\mathbf{r})$ is the optical potential which describes the interaction taking place between the N^* resonance and nucleus. $\Gamma_{N^*}(m)$ denotes the total width of N^* for its mass equal to m. It consists of the partial decay widths due to the $N^* \to N\pi(\sim 40\%)$, $N^* \to N\eta(\sim 50\%)$ and $N^* \to N\pi\pi(\sim 10\%)$ [9, 22]:

$$\Gamma_{N^*}(m) \approx \Gamma_{N^*}(m_{N^*}) \left[0.4\frac{k_\pi(m)}{k_\pi(m_{N^*})} + 0.5\frac{k_\eta(m)}{k_\eta(m_{N^*})} + 0.1\right]; \quad \Gamma_{N^*}(m_{N^*}) = 0.15 \text{ GeV}. \tag{9}$$

In this equation, $k_{\pi(\eta)}(m)$ is the pseudoscalar meson momentum arising due to the N^* of mass m decaying at rest. It can be evaluated using the equation:

$$k_M(m) = \frac{[(m^2 - (m_N + m_M)^2)(m^2 - (m_N - m_M)^2)]^{1/2}}{2m}; \qquad (M = \pi^0, \eta). \tag{10}$$

The differential cross section for the reaction illustrated above is given by

$$\frac{d\sigma}{dE_{p'}d\Omega_{p'}d\Omega_\eta} = K_F < |T_{fi}|^2 >, \tag{11}$$

where the annular brackets around $|T_{fi}|^2$ represent the average over the spins in the initial state and the summation over the spins in the final state. K_F is the kinematical factor for the reaction:

$$K_F = \frac{\pi}{(2\pi)^6}\frac{m_p^2 m_A k_{p'} k_\eta^2}{k_p|k_\eta(E_i - E_{p'}) - E_\eta \mathbf{q}.\hat{k}_\eta|}. \tag{12}$$

All symbols carry their usual meanings.

3 Results and Discussions

The optical potential $V_{OX}(\mathbf{r})$, appearring in the N^* propagator $G_{N^*}(m,\mathbf{r})$ in Eq. (8) and the distorted wave functions χs in Eqs. (6) and (7), is calculated using the "$t\varrho(\mathbf{r})$" approximation [21, 23], i.e.,

$$V_{OX}(\mathbf{r}) = -\frac{v_X}{2}[i+\alpha_{XN}]\sigma_t^{XN}\varrho(\mathbf{r}), \tag{13}$$

where the symbol X stands for the proton or $N^*(1535)$ resonance. v_X is the velocity of the particle X. α_{XN} denotes the ratio of the real to imaginary part of the scattering amplitude f_{XN}. σ_t^{XN} represents the corresponding total cross section. To evaluate the proton nucleus optical potential, i.e., $V_{Op}(\mathbf{r})$ as well as $V_{Op'}(\mathbf{r})$, we use the energy dependent experimentally determined values for α_{pN} and σ_t^{pN} [24]. The measured values for the N^* nucleon scattering parameters α_{N^*N} and $\sigma_t^{N^*N}$ are not available. To estimate them, we take $\alpha_{N^*N} \approx \alpha_{pN}$ and $\sigma_{el}^{N^*N} \approx \sigma_{el}^{pN}$ since the elastic scattering dynamics of the N^* resonance can be assumed not much different compare to that of a proton [25]. The reactive or inelastic part of the total cross section, i.e., $\sigma_{in}^{N^*N}$, should be negligible [25] according to reciprocity theorem, as the cross section $\sigma_t(pp \to pN^*)$ is very small [26]. Therefore, we take $\sigma_t^{N^*N} \approx \sigma_{el}^{pN}$. The η meson nucleus optical potential $V_{O\eta}$ $(\mathbf{r})$ can be estimated from the η meson self-energy Π_η $(\mathbf{r})$ in the nucleus evaluated by Alvaredo and Oset [17]:

$$\Pi_\eta(\mathbf{r}) = 2E_\eta V_{O\eta}(\mathbf{r}) = g_\eta^{*2}\frac{\varrho(\mathbf{r})}{m - m_{N^*} + \frac{i}{2}\Gamma_{N^*}(m) - V_{ON^*}(\mathbf{r}) + V_{ON}(\mathbf{r})}, \tag{14}$$

where the nucleon potential energy is taken as $V_{ON}(\mathbf{r}) = -50\varrho(\mathbf{r})/\varrho(0)$ MeV [17].

The factor $\varrho(\mathbf{r})$, appearing in Eqs. (3), (13) and (14), represents the spatial density distribution of the nucleus. The form of $\varrho(\mathbf{r})$ for ^{14}C nucleus, as extracted from the electron scattering data [27], is given by

$$\varrho(\mathbf{r}) = \varrho_0[1 + w(r/c)^2]e^{-(r/c)^2}; \quad w = 1.38,\ c = 1.73 \text{ fm}. \tag{15}$$

This density distribution is normalized to the mass number of the nucleus.

We present in Fig. 2 the calculated differential cross section $\frac{d\sigma}{dE_{p'}d\Omega_{p'}d\Omega_\eta}$ of the energy transfer $q_0(= E_p - E_{p'})$ distribution for the coherent η meson production in the (p,p') reaction on ^{14}C at 2.25, 2.5, and 3.0 GeV. This figure shows that the contribution to the cross section from the π^0 meson exchange interaction (dot-dashed curve) is much larger than that of the η meson exchange interaction (dashed curve). Depending on the beam energy, the cross section at the peak due to the π^0 meson exchange interaction is $5-8$ times larger and the peak positions due to it appear at about $140-220$ MeV lower value

of q_0 in compare to those due to the η meson exchange interaction. This figure also shows that the cross sections are enhanced significantly (solid curve) due to the interference of these interactions. As shown in this figure, the peak cross section due to the coherent π^0 and η meson exchange interactions is $10-14$ times larger and the peak positions appear at about $100-170$ MeV lower value of q_0 in compare to those due to the η meson exchange interaction. In addition to these, Fig. 2 also shows that the cross section strongly depends on the beam energy. The overall cross section at the peak enhances from ~ 0.11 (mb/GeVsr^2) at 2.25 GeV to 0.29 (mb/GeVsr^2) at 3.0 GeV. With the increase in the beam energy, the peak position is shifted by 70 MeV towards the higher value of q_0.

The dominancy of the pion exchange interaction over that of the η meson can easily be understood by analysizing the coupling constants, form factors, and virtual meson propagators in the T_{fi}-matrix (see Eq. (3)). $|T_{fi}|^2$, as shown in Eq. (11), appears in the differential cross section. The values of the coupling constants, quoted below Eq. (1), show the ratio $|g_\pi g_\pi^*/g_\eta g_\eta^*|^2$ is approximately equal to 0.37. For ^{14}C nucleus at 2.5 GeV, the form factors (at the respective peaks) in Eq. (2) are $F_\pi(q^2 \simeq -0.089 \text{ GeV}^2) = F_\pi^*(q^2 \simeq -0.089 \text{ GeV}^2) = 0.94$ and $F_\eta(q^2 \simeq -0.133 \text{ GeV}^2) = F_\eta^*(q^2 \simeq -0.133 \text{ GeV}^2) = 0.82$. They give $|F_\pi(q^2)/F_\eta(q^2)|^4 \approx 1.73$. This factor multiplied by $|g_\pi g_\pi^*/g_\eta g_\eta^*|^2$ leads to a factor close to 0.64. The values of the pseudoscalar meson propagators are $G_\pi(q^2 \simeq -0.089 \text{ GeV}^2) = -9.35 \text{ GeV}^{-2}$ and $G_\eta(q^2 \simeq -0.133 \text{ GeV}^2) = -2.31 \text{ GeV}^{-2}$, which show $|G_\pi(q^2)/G_\eta(q^2)|^2 \approx 16.38$. The relatively larger values for F_π (compare to F_η) and G_π (compare to G_η) arise since the mass of the π^0 meson is much less than that of the η meson. This analysis shows that the cross section due to the pion exchange interaction should be significantly larger than that due to the η meson exchange interaction.

Fig. 3 describes the dependence of the calculated cross section on the $N^*(1535)$ nucleus potential V_{ON^*} at 2.5 GeV for the ^{14}C nucleus. The incorporation of V_{ON^*} in the calculation, as shown in this figure, reduces the cross section at the peak from 0.18 mb/GeVsr^2 (dot-dot-dashed curve) to 0.16 mb/GeVsr^2 (solid curve), i.e., the reduction in the cross section is about 11.28%. In addition, the incorporation of this potential shifts the peak position from $q_0 = 900$ MeV to $q_0 = 920$ MeV. At the peak, the energy of the N^* resonance E_{N^*} (in the laboratory frame) is found equal to 1.85 GeV, and the optical potential for it is $V_{ON^*}(0) = (-10.96, -18.55)$ MeV.

We describe the sensitivity of the calculated cross section to the η meson nucleus optical potential $V_{O\eta}$ in Fig. 4. This figure shows that the inclusion of $V_{O\eta}$ in the calculation decrease the peak cross section significantly, i.e., by 22.81%. This potential reduces the cross section at the peak from ~ 0.21 mb/GeVsr^2 (dot-dot-dashed curve) to 0.16 mb/GeVsr^2 (solid curve), and it shifts the peak position from $q_0 = 900$ MeV to $q_0 = 920$ MeV. At the peak, $E_\eta \simeq 918$ MeV, the η meson nucleus optical potential is $V_{O\eta}(0) = (13.14, -16.17)$ MeV.

The effects of the initial and final state interactions on the cross section for the energy

transfer q_0 distribution spectrum are illustrated in Fig. 5. In all results presented in this figure, the $N^*(1535)$ nucleus optical potential V_{ON^*} is included. The plane wave result is shown by the dashed curve where the peak appears at $q_0 = 970$ MeV and the magnitude of the cross section at the peak is 1.79 mb/GeVsr^2. The initial state interaction ISI, i.e., the beam proton and nucleus interaction, reduces the peak cross section to ~ 0.52 mb/GeVsr^2 (dot-dashed curve), and it shifts its position at $q_0 = 930$ MeV. The final state interaction FSI, i.e., the interactions of both p' and η meson with the recoiling nucleus, reduces further the cross section (solid curve) to 0.16 mb/GeVsr^2 at the peak which appears at $q_0 = 920$ MeV.

4 Conclusions

We have calculated the differential cross sections for the energy transfer distribution of the coherent η meson production in the proton nucleus reaction. The η meson in the final state appears due to the decay of $N^*(1535)$ produced in the intermediate state. The N^* excitation is occurred due to the π^0 and η meson exchange interactions. The contribution of the pion exchange interaction to the cross section is much larger than that of the η meson exchange interaction. The interference of these interactions increases the cross section significantly. The reduction in the cross section due to the N^* nucleus potential is less than that due to the η meson nucleus potential. Both of these potentials shift the peak position towards the higher value of the energy transferred q_0 to the nucleus. Compare to the plane wave results, the initial and final state interactions shift the peak position towards the lower value of q_0, and they drastically reduce the cross section at the peak.

5 Acknowledgement

The author gratefully acknowledge Dr. A. Chatterjee (Head, Nuclear Physics Division) for his support and encouragement.

References

[1] B. Höistad et al., arXiv/nucl-th:0610011.

[2] S. Schadmand (for WASA at COSY Collaboration), Pramana **75** (2010) 225.

[3] J. Berger et al., Phys. Rev. Lett. **61** (1988) 919; R. Frascaria et al., Phys. Rev. C **50** (1994) R537.

[4] J. C. Peng et al., Phys. Rev. Lett. **63** (1989) 2353.

[5] W. B. Tippens et al., Phys. Rev. D **63** (2001) 052001.

[6] F. -D. Berg et al., Phys. Rev. Lett. **72** (1994) 977.

[7] M. Williams et al., Phys. Rev. C **80** (2009) 045213; B. Krusche et al., Phys. Rev. Lett. **74** (1995) 3736; J. W. Price et al., Phys. Rev. C **51** (1995) R2283; B. Krusche et al., Phys. Lett. B **358** (1995) 40; M. Röbig-Landau et al., Phys. Lett. B **373** (1996) 45.

[8] Q. Haider and L. C. Liu, Phys. Lett. B **172** (1986) 257; L. C. Liu and Q. Haider, Phys. Rev. C **34** (1986) 1845; G. L. Li, W. K. Cheng and T. T. S. Kuo, Phys. Lett. B **195** (1987) 515.

[9] H. C. Chiang, E. Oset and L. C. Liu, Phys. Rev. C **44** (1991) 738.

[10] R. E. Chrien et al., Phys. Rev. Lett. **60** (1988) 2595; A. Budzanowski et al., (COSY-GEM Collaboration), Phys. Rev. C **79** (2009) 012201(R); ibid, **82** (2010) 041001(R).

[11] C. Y. Cheung, Phys. Lett. B **119** (1982) 47; ibid, **138** (1984) 245; C. Wilkin, Phys. Lett. B **331** (1994) 276.

[12] J. Lehr, M. Post and U. Mosel, Phys. Rev. C **68** (2003) 044601; J. Lehr, U. Mosel, ibid, 044603; R. C. Carrasco, ibid, **48** (1993) 2333.

[13] M. Hedayati-Poor and H. S. Sherif, Phys. Rev. C **76** (2007) 055207; M. Hedayati-Poor, S. Bayegan and H. S. Sherif, Phys. Rev. C **68** (2003) 045205.

[14] Ch. Sauerman, B. L. Friman and W. Nörenberg, Phys. Lett. B **341** (1995) 261; L. -C. Liu, J. T. Londergan and G. E. Walker, Phys. Rev. C **40** (1989) 832; J. -F. Germond and C. Wilkin, Nucl. Phys. A **518** (1990) 308; A. Moalem, E. Gedalin, L. Razdolskaja and Z. Shorer, Nucl. Phys. A **589** (1995) 649.

[15] J. M. Laget, F. Wellers and J. F. Lecolley, Phys. Lett. B **257** (1991) 254.

[16] T. Vetter, A Engel, T. Brió and U. Mosel, Phys. Lett. B **263** (1991) 153.

[17] B. Lopez Alvaredo and E. Oset, Phys. Lett. B **324** (1994) 125.

[18] T. Ericson and W. Weise, Pions and Nuclei (Clarendon Press, Oxford, 1988).

[19] R. Machleidt, K. Holinde and Ch. Elster, Phys. Rep. **149** (1987) 1.

[20] R. J. Glauber, in Lectures in theoretical physics, vol. 1, edited by W. E. Brittin et al., (Interscience Publishers, New York, 1959).

[21] S. Das, Phys. Rev. C **72** (2005) 064619.

[22] G. Fäldt and C. Wilkin, Nucl. Phys. A **587** (1995) 769.

[23] S. Das, Phys. Rev. C **83** (2011) 064608.

[24] D. V. Bugg, et al., Phys. Rev. **146** (1966) 980; S. Barshay, et al., Phys. Rev. C **11** (1975) 360; W. Grein, Nucl. Phys. B **131** (1977) 255; C. Lechanoine-Leluc and F. Lehar, Rev. Mod. Phys. **65** (1993) 47; R. M. Barnett et al., Particle Data Group, Phys. Rev. D **54**, (1996) 192; http://pdg.lbl.gov/xsect/contents.html.

[25] A. B. Santra and B. K. Jain, Nucl. Phys. A **634** (1998) 309.

[26] Baldini et al., Landolt-Berrnstein Vol. 12 (Springer, Berlin, 1987); E. Chiavassa et al., Phys. Lett. B **322** (1994) 270.

[27] C. W. De Jager, H. De. Vries and C. De Vries, At. Data Nucl. Data Tables, **14** (1974) 479.

Figure Captions

1. (color online). Schematic diagram of the elementary reaction: $pN \to p'N^*$; $N^* \to N\eta$.

2. (color online). The energy transfer $q_0(= E_p - E_{p'})$ distribution spectra for the ^{14}C nucleus at 2.25, 2.5 and 3.0 GeV. The contribution due to the π^0 meson exchange interaction is shown by the dot-dashed curve whereas the dashed curve represents the contribution due to the η meson exchange interaction. The cross section due to these interactions along with their interference is illustrated by the solid curve.

3. (color online). The dependence of the calculated cross section on the $N^*(1535)$ nucleus potential V_{ON^*}. This potential reduces the cross section by 11.28% and shifts the peak position by 20 MeV towards the higher energy transfer q_0.

4. (color online). The sensitivity of the cross section to the η meson nucleus potential $V_{O\eta}$. This potential reduces the cross section at the peak by 22.81% and shifts the peak position by 20 MeV towards the larger energy transfer q_0.

5. (color online). The effect of ISI (initial state interaction) and FSI (final state interaction) on the calculated cross section (see text). In these results, the $N^*(1535)$ interaction with the nucleus, i.e., V_{ON^*}, is taken into account.

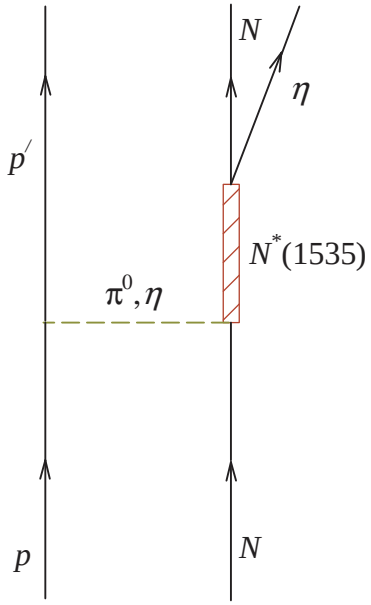

Fig.1

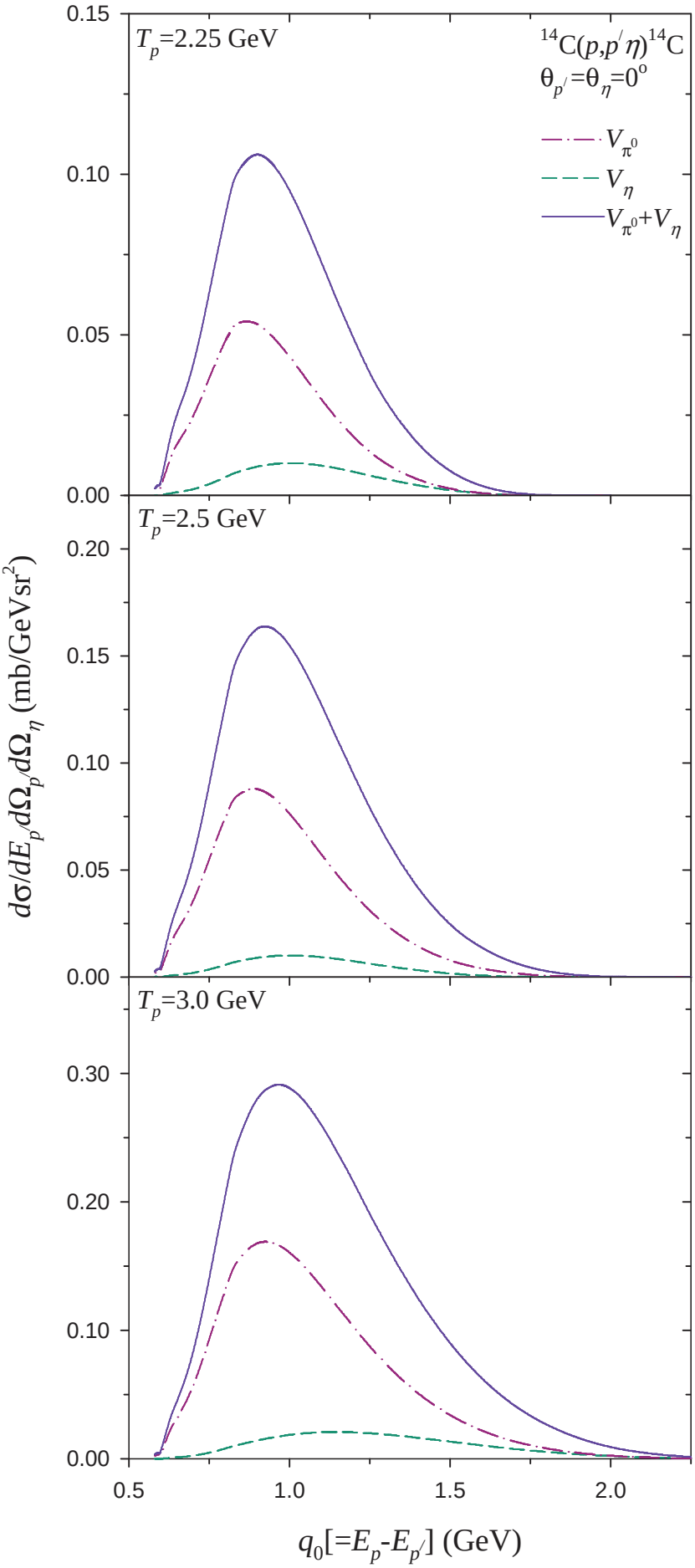
T_p=2.25 GeV
^{14}C(p,$p'\eta$)^{14}C
$\theta_{p'}=\theta_\eta=0^o$
V_{π^0}
V_η
$V_{\pi^0}+V_\eta$
T_p=2.5 GeV
T_p=3.0 GeV
$d\sigma/dE_{p'}d\Omega_{p'}d\Omega_\eta$ (mb/GeVsr^2)
$q_0[=E_p-E_{p'}]$ (GeV)
0.00
0.05
0.10
0.15
0.20
0.30
0.5
1.0
1.5
2.0

Fig. 2

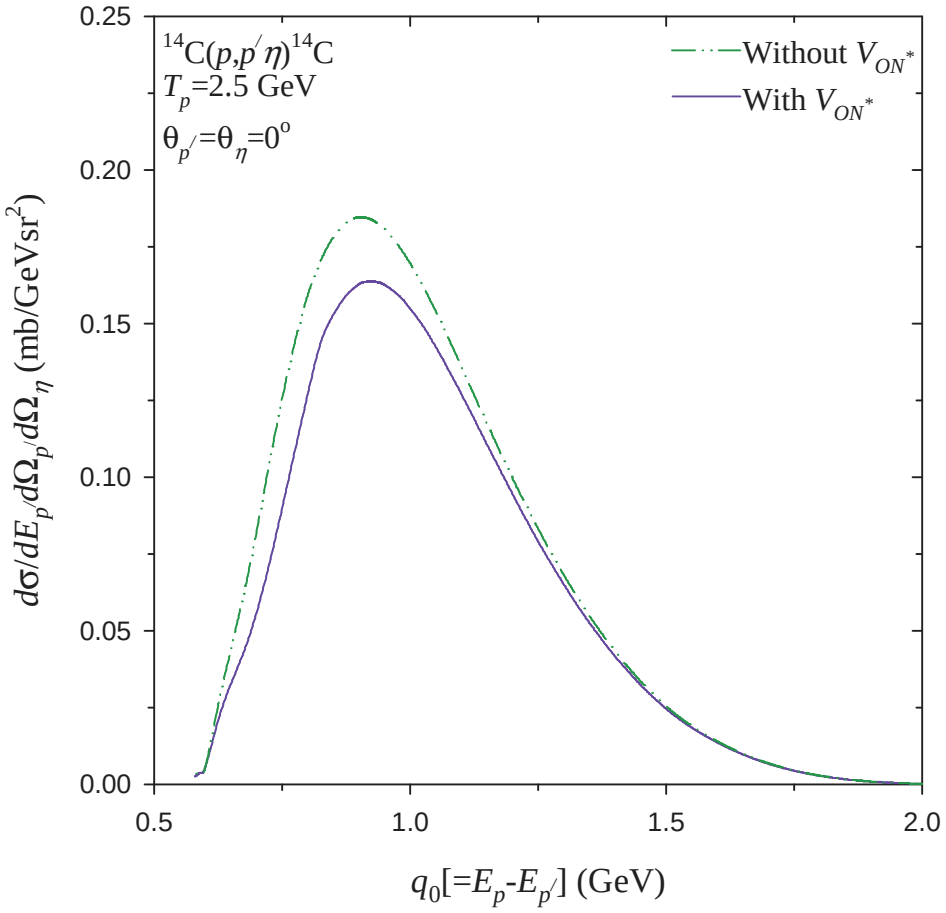
^{14}C(p,$p'\eta$)^{14}C
T_p=2.5 GeV
$\theta_{p'}=\theta_\eta=0^o$
Without V_{ON^*}
With V_{ON^*}
$d\sigma/dE_{p'}d\Omega_{p'}d\Omega_\eta$ (mb/GeVsr^2)
$q_0[=E_p-E_{p'}]$ (GeV)
0.25
0.20
0.15
0.10
0.05
0.00
0.5
1.0
1.5
2.0

Fig. 3

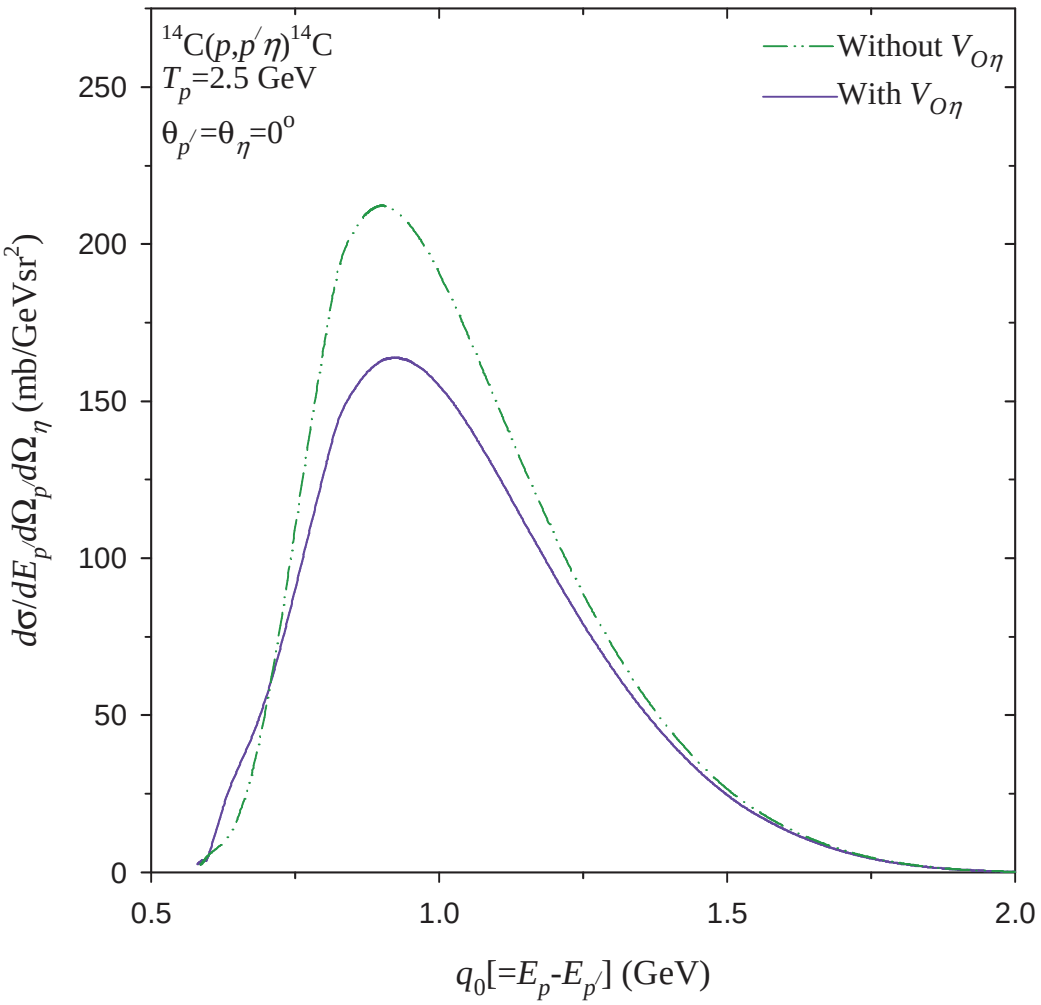
^{14}C(p,$p'\eta$)^{14}C
T_p=2.5 GeV
$\theta_{p'}=\theta_\eta=0^o$
Without $V_{O\eta}$
With $V_{O\eta}$
$d\sigma/dE_{p'}d\Omega_{p'}d\Omega_\eta$ (mb/GeVsr^2)
0
50
100
150
200
250
0.5
1.0
1.5
2.0
q_0[=E_p-$E_{p'}$] (GeV)

Fig.4

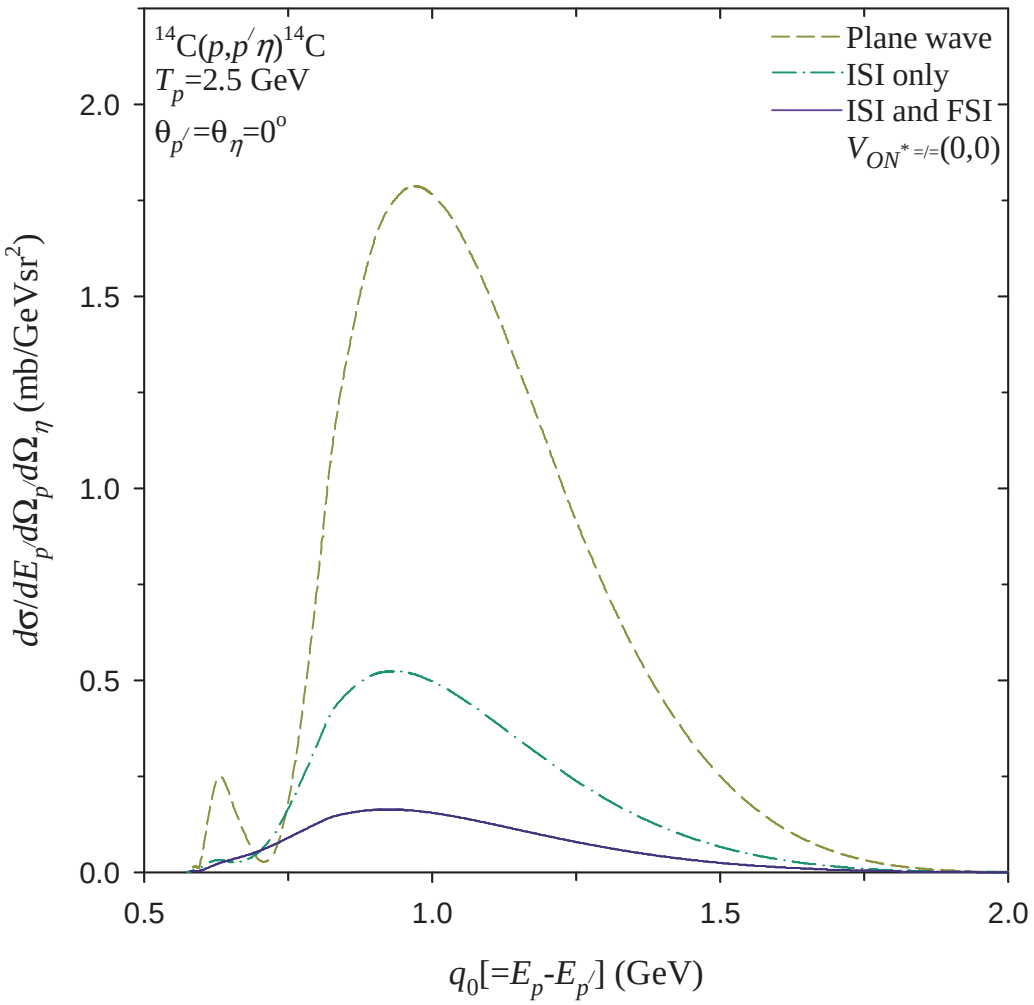
^{14}C(p,$p'\eta$)^{14}C
T_p=2.5 GeV
$\theta_{p'}=\theta_\eta=0^o$
Plane wave
ISI only
ISI and FSI
$V_{ON^*=/=}$(0,0)
$d\sigma/dE_{p'}d\Omega_{p'}d\Omega_\eta$ (mb/GeVsr^2)
$q_0[=E_p-E_{p'}]$ (GeV)
0.0
0.5
1.0
1.5
2.0
0.5
1.0
1.5
2.0

Fig. 5